İstanbul Commerce University Journal of Science, 20(39), Spring 2021, 35-56.

İSTANBUL TİCARET ÜNİVERSİTESİ
FEN BİLİMLERİ DERGİSİ

İstanbul Commerce University Journal of Science

http://dergipark.gov.tr/ticaretfbd

Research Article / Araştırma Makalesi

ESTIMATING DOMINANT PARAMETERS OF AIRCRAFT LINEAR DYNAMICAL MODEL VIA LEAST SQUARE METHOD

EN KÜÇÜK KARELER YÖNTEMİ İLE DOĞRUSAL DİNAMİK UÇAK MODELİNİN DOMİNANT PARAMETRELERİNİN TAHMİN EDİLMESİ

Mehmet ŞAHİN[1] **Muammer KALYON**[2]

Corresponding Author / Sorumlu Yazar
mehmet.sahin3@tai.com.tr

Received / Geliş Tarihi
07.05.2021

Accepted / Kabul Tarihi
03.06.2021

Abstract

Parameter estimation methods are used to create mathematical models for systems with input and output. In this article, the least squares method (LS) for aircraft is proposed. This method is used to write a realistic equation of the mathematical relationship between physical quantities that vary depending on each other. The parameters of the transfer functions formed as a result of the aircraft mathematical model were estimated with the LS method. Thus, the algorithm of the LS method was created and the results obtained in the MATLAB/Simulink program were shared. As a result of the estimated transfer functions, some aerodynamic coefficients are estimated. In addition, the Integral Square Error (ISE) table has been extracted to see the approximation of the LS method to the real data. this table is also created for transfer functions and aerodynamic parameters. Thus, the error rate of the method was observed.

Keywords: Aerodynamic parameters, aircraft control surfaces, Least Square (LS) method, parameter estimation, system identification.

Öz

Girişi ve bu girişe göre çıkışı olan sistemlere matematiksel model oluşturmak için parametre tahmin metodları kullanılmaktadır. Bu makalede, hava aracında kullanılmak üzere tahmin metodu olan en küçük kareler metodu (LS) önerilmektedir. Bu yöntem, birbirine bağlı olarak değişen iki fiziksel büyüklük arasındaki matematiksel bağlantıyı, gerçeğe uygun bir denklem olarak yazmak için kullanılır. LS metodu kullanılarak hava aracı matematiksel modeli neticesinde oluşan transfer fonksiyonlarının parametreleri tahmin edilerek çıkarılmıştır. Böylece LS metodunun algoritması çıkarılmış ve MATLAB/Simulink programında elde edilen sonuçlar paylaşılmıştır. Ayrıca tahmin edilmiş transfer fonksiyonları neticesinde bazı aerodinamik katsayılar tahmin edilmiştir. Son olarak LS metodunun gerçek verilere yaklaşımını görmek için İntegral Kare Hatası (ISE) tablosu çıkarılmıştır. ISE tablosu tahmin edilen transfer fonksiyonları ve aerodinamik katsayılar için oluşturulmuştur. Böylece metodun hata oranı gözlemlenmiştir.

Anahtar Kelimeler: Aerodinamik parametreler, En Küçük Kareler (LS) Metodu, parametre tahmini, sistem tanımlama, uçak kontrol yüzeyleri.

This publication was produced from the Master thesis of Mehmet ŞAHİN in the Mechatronics Engineering Program of Istanbul Commerce University, Institute of Science and Technology.

[1]İstanbul Commerce University, Institute of Science and Technology, Department of Mechatronics Engineering, Küçükyalı, İstanbul, Turkey.
mehmet.sahin3@tai.com.tr, Orcid.org/0000-0001-9399-8559.

[2]İstanbul Commerce University, Engineering Faculty, Department of Mechatronics Engineering, Küçükyalı, İstanbul, Turkey.
mkalyon@ticaret.edu.tr, Orcid.org/0000-0002-8168-2773.

1. INTRODUCTION

Systems are structures with input and output based on specific measurements and observations. If the defined input and output values exist, the current system definition process continues. System identification is a discipline that provides the most suitable representation for a system and answers to the inverse problem when its behavior is examined as a result of many observations (Jategaonkar, 2006). The inverse problem, namely the system identification, has been a fundamental element of defining any system under consideration and having the knowledge to examine that system. As we have explained the system, is a physical system with inputs and outputs in aircraft. System identification procedures perform the process of estimating the mathematical model of this physical system.

Aviation is one of the areas where system identification is most commonly used. System identification is employed in aerospace, such as flight performance analysis, estimation of aircraft parameters, and air vehicle models/submodels verification. It may be stated that system identification in aerospace intends to investigate the behavior of the aircraft via flight test data.

There is more than one method used in this context. One of them is the least squares method described in this paper. The data gathered by any application in real life is analyzed in a tabular form, and a function that models the collected data is tried to be found. It is often difficult to find a function that fits this data sheet exactly; The function that best fits the data table is tried to be determined. Regression analysis is an analysis method used to measure the relationship between two or more quantitative variables. One of the most used techniques in regression analysis is the least squares method. In this paper, LS methods are explained, and The estimation process of some parameters in transfer functions obtained as a result of the mathematical model of an aircraft is explained. It has been observed to what extent LS methods give results. The original data were compared with the LS method, and graphs were acquired in the time domain for each control surface to measure the accuracy of the results. After the transfer functions were evaluated, the estimation of some aerodynamic coefficients using the LS method's predicted values was also performed by the functions. A table compared with the values taken initially as the basis is specified in this context. An integral Square Error (ISE) table has been prepared to show how accurately it is estimated between this method and the original data.

2. MATHEMATICAL MODEL OF AIRCRAFT

The aircraft system identification is involved with implementing a mathematical expression for aerodynamic forces and moments in terms of relevant, measurable quantities such as control surface deviations, aircraft angular velocities, airspeed, or Mach number. Aerodynamic parameters characterize the interdependence of aerodynamic forces and moments on measurable quantities when the mathematical model is parametric. It is crucial to have a mathematical model of the aircraft to compute the parameters. The mathematical model of the aircraft also covers both equations of motion and equations for aerodynamic forces and moments recognized as aerodynamic equations. The traditional aircraft control and simulation book was used to create a mathematical model of an aircraft (Stevens, Lewis and Johnson, 2016). Again, the system identification book for conventional aircraft was used in mathematical model formation and system identification (Klein and Morielli, 2006). Figure 1 presents the components on the aircraft related to the notation that will be interpreted in this section.

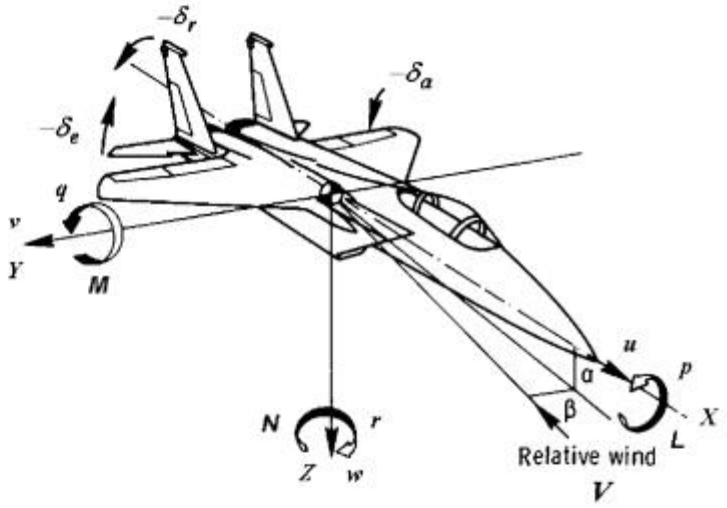

Figure 1. u, v, w = body-axis components of aircraft velocity relative to Earth axes; p, q, r = body-axis components of aircraft angular velocity; X, Y, Z = body-axis components of aerodynamic force acting on the aircraft; and L, M, N = body-axis components of aerodynamic moment acting on the aircraft (Morielli and Klein, 2006)

2.1. Aircraft Equation and Motion

The general motion is revealed as Equations (1) and (2) in the forms of translation and rotation by Newton's second law of motion.

$$F = \frac{d}{dt}(mV) \tag{1}$$

$$M = \frac{d}{dt}(I\omega) \tag{2}$$

where F is the force, mV is the linear momentum, m is the mass, V is the translational velocity, M is the moment, $I\omega$ is the angular momentum, ω is the angular velocity, and I is the inertia matrix. Equations 1 and 2 are vector equations describing translation and rotational motion. Each vector equation expresses three scalar Equations for vector components. Thus, six scalar Equations are formed for six degrees of freedom for aircraft motion. Below, the body axis components of the force, velocity, moment and angular velocity expressions in Equations 1 and 2 are specified in $F = [F_x \quad F_y \quad F_z]^T$, $V = [u \quad v \quad w]^T$, $M = [M_x \quad M_y \quad M_z]^T$, $\omega = [p \quad q \quad r]^T$.

Thus, the angular momentum expression is specified in Equation (3) to be used to find moment Equations.

$$I\omega = \begin{bmatrix} I_{xx} & -I_{xy} & -I_{xz} \\ -I_{yx} & I_{yy} & -I_{yz} \\ -I_{xz} & -I_{yz} & I_{zz} \end{bmatrix} \begin{bmatrix} p \\ q \\ r \end{bmatrix} \rightarrow I\omega = \begin{bmatrix} I_x p - I_{xz} r \\ I_y q \\ -I_{xz} p + I_z r \end{bmatrix} \tag{3}$$

I inertia matrix symmetric matrix, where $I_{xy} = I_{yx} = I_{yz} = I_{zy} = 0$.

Equations (4) and (5) are formed by combining Equations (1) and (2). These equations are vector forms of the equations of motion expressed on the body axis.

$$F = m\dot{V} + \omega \times mV \quad (4)$$

$$M = I\dot{\omega} + \omega \times I\omega \quad (5)$$

In the framework of the expression in Equation (1) and (2), when the components of Equation (3) and body axis are put into Equation (4) and (5), the components of force and moment equations in Equation (6) and (7) are found.

Force Equations:

$$\begin{aligned} F_x &= m(\dot{u} + qw - rv) \\ F_y &= m(\dot{v} + ru - pw) \\ F_z &= m(\dot{w} + pv - qu) \end{aligned} \quad (6)$$

Moment Equations:

$$\begin{aligned} M_x &= \dot{p}I_x - \dot{r}I_{xz} + qr\left(I_z - I_y\right) - qpI_{xz} \\ M_y &= \dot{q}I_y + pr(I_x - I_z) + (p^2 - r^2)I_{xz} \\ M_z &= \dot{r}I_z + \dot{p}I_{xz} + pq\left(I_y - I_x\right) + qrI_{xz} \end{aligned} \quad (7)$$

For aircraft, the forces and moments of the previous equations consist of aerodynamics, gravity, and thrust. Thus, Equations (4) and (5) are expressed as Equations (8) and (9) as follows.

$$\underbrace{F_A + F_T + F_G}_{\sum F} = m\dot{V} + \omega \times mV \quad (8)$$

$$M_A + M_T = I\dot{\omega} + \omega \times I\omega \quad (9)$$

Components of aerodynamic forces and moments affecting the aircraft are shown in Equations (10) and (11).

$$F_A = \bar{q}S \begin{bmatrix} C_x \\ C_y \\ C_z \end{bmatrix} \quad (10)$$

$$M_A = \bar{q}S \begin{bmatrix} bC_l \\ cC_m \\ bC_n \end{bmatrix} \quad (11)$$

where $\bar{q} = 0.5\rho V^2$ is the dynamic pressure, V is the airspeed, ρ is the air density, S is the wing area, b is the wing span, and c is the chord length. In Equation (12), (13) and (14) expressed component of gravity, thrust force and thrust moment vector.

$$F_G = \begin{bmatrix} -mgsin\theta \\ mgcos\theta sin\phi \\ mgcos\theta cos\phi \end{bmatrix} \quad (12)$$

$$F_T = \begin{bmatrix} T \\ 0 \\ 0 \end{bmatrix} \tag{13}$$

$$M_T = \begin{bmatrix} 0 \\ 0 \\ 0 \end{bmatrix} \tag{14}$$

Hence, aerodynamic forces and moments are presented in Equations (15) and (16).

Force Equations:

$$\begin{aligned} m\dot{u} &= m(rv - qw) + \bar{q}SC_x - mgsin\theta + T \\ m\dot{v} &= m(pw - ru) + \bar{q}SC_y + mgcos\theta sin\phi \\ m\dot{w} &= m(qu - pv) + \bar{q}SC_z + mgcos\theta cos\phi \end{aligned} \tag{15}$$

Moment Equations:

$$\begin{aligned} \dot{p}I_x - \dot{r}I_{xz} &= \bar{q}SbC_l - qr(I_z - I_y) + qpI_{xz} \\ \dot{q}I_y &= \bar{q}ScC_m - pr(I_x - I_z) - (p^2 - r^2)I_{xz} + I_p\Omega_p r \\ \dot{r}I_z - \dot{p}I_{xz} &= \bar{q}SbC_n - pq(I_y - I_x) - qrI_{xz} - I_p\Omega_p q \end{aligned} \tag{16}$$

2.2. Rotational Kinematic Equations

Rotational kinematic equations connect the rate of change of Euler angles to the body axis relation of angular velocity and it is expressed in Equation (17).

$$\begin{bmatrix} p \\ q \\ r \end{bmatrix} = \begin{bmatrix} 1 & 0 & -\sin\theta \\ 0 & \cos\Phi & \sin\Phi cos\theta \\ 0 & -\sin\Phi & cos\Phi cos\theta \end{bmatrix} \begin{bmatrix} \dot{\Phi} \\ \dot{\theta} \\ \dot{\psi} \end{bmatrix} \tag{17}$$

2.3. The Linearized Equations of Motion

Highly nonlinear Equations are linearized to easily investigate aircraft motions and behaviors (Blakelock, 1991). In this section, the linearization of the plane motion equations for both longitudinal and lateral motion is described to reveal the transfer functions to be analyzed for the system identification process detailed as follows. As a result of linearization, transfer functions will be obtained without any complexity, and system definition will be implemented more efficiently.

2.3.1. The linearized longitudinal equations

States of the longitudinal motions that are aircraft velocity (v_p), angular velocity pitch component (q), pitch angle (θ) and angle of attack (α). Before performing the linearization process, the nonlinear forms of the state are given in Equation (18-20).

$$\dot{V_p} = \frac{-0.5\rho\left(V_{p_0}+v_p\right)^2 SC_D}{m} + \left(\frac{P_x}{m} - gsin\theta\right)cos\alpha + \left(\frac{P_z}{m} + gcos\theta\right)sin\alpha \tag{18}$$

$$\dot{\alpha} = q - \frac{-0.5\rho\left(V_{p_0}+v_p\right)S(C_L)}{m} + \frac{g}{V_{p_0}+v_p} - \frac{P_x\alpha}{m\left(V_{p_0}+v_p\right)} + \frac{P_z}{m\left(V_{p_0}+v_p\right)} \tag{19}$$

$$\dot{q} = \frac{-0.5\rho\left(V_{p_0}+v_p\right)^2 Sc(C_{M_0}+C_{M_\alpha}+C_M)}{I_{yy}} + \frac{-0.5\rho\left(V_{p_0}+v_p\right)ScC_M}{I_{yy}} \tag{20}$$

For linearization the equilibrium points of states are $v_p = V_{p_0}$, $\alpha = \alpha_0 = 0$, $\theta = \theta_0 = 0$ and $q = 0$. Thus, the linearized longitudinal motion equations for $\dot{V}_p$, $\dot{\alpha}$, $\dot{q}$, $\dot{\theta}$ are expressed in Equation (21-24).

$$\dot{V}_p = \frac{-2g(C_{D_0}+C_{D_{CL^2}}C_{L_0}{}^2)}{V_{p_0}C_L} v_p + g\left(1 - 2C_{D_{CL^2}}\frac{C_{L_0}}{C_L}C_{L_\alpha} + \frac{P_z}{m}\right)\alpha - g\theta \tag{21}$$

$$\dot{\alpha} = \frac{-g}{V_{p_0}{}^2}\left(1 + \frac{C_{L_0}}{C_L} + \frac{P_z}{mg}\right)v_p - \left(\frac{g}{V_{p_0}}\frac{C_{L\alpha}}{C_L} + \frac{P_x}{mV_{p_0}}\right)\alpha - \frac{g}{V_{p_0}}\frac{C_{L_{\delta_e}}}{C_L}\delta_e + q \tag{22}$$

$$\dot{q} = \frac{2mgcC_{M_0}}{I_{yy}V_{p_0}C_L}v_p + \frac{mgcC_{M\alpha}}{I_{yy}C_L}\alpha + \frac{mgc^2C_{M\dot{\alpha}}}{2I_{yy}V_{p_0}C_L}\dot{\alpha} + \frac{mgc^2C_{M_Q}}{2I_{yy}V_{p_0}C_L}q + \frac{mgcC_{M_{\delta_e}}}{I_{yy}C_L}\delta_e \tag{23}$$

$$\dot{\theta} = q \tag{24}$$

These equations are specified in the form of vector notation in Equation (25) as follows.

$$C\dot{X} = AX + B\delta_e \rightarrow \begin{bmatrix} 1 & 0 & 0 & 0 \\ 0 & 1 & 0 & 0 \\ 0 & c_{32} & 1 & 0 \\ 0 & 0 & 0 & 1 \end{bmatrix}\begin{bmatrix} \dot{v}_p \\ \dot{\alpha} \\ \dot{q} \\ \dot{\theta} \end{bmatrix} = \begin{bmatrix} a_{11} & a_{12} & 0 & -g \\ a_{21} & a_{22} & 1 & 0 \\ a_{31} & a_{32} & a_{33} & 0 \\ 0 & 0 & 1 & 0 \end{bmatrix}\begin{bmatrix} v_p \\ \alpha \\ q \\ \theta \end{bmatrix} + \begin{bmatrix} 0 \\ b_2 \\ b_3 \\ 0 \end{bmatrix}\delta_e \tag{25}$$

where,

$$C = \begin{bmatrix} 1 & 0 & 0 & 0 \\ 0 & 1 & 0 & 0 \\ 0 & c_{32} & 1 & 0 \\ 0 & 0 & 0 & 1 \end{bmatrix}, A = \begin{bmatrix} a_{11} & a_{12} & 0 & -g \\ a_{21} & a_{22} & 1 & 0 \\ a_{31} & a_{32} & a_{33} & 0 \\ 0 & 0 & 1 & 0 \end{bmatrix}, B = \begin{bmatrix} 0 \\ b_2 \\ b_3 \\ 0 \end{bmatrix}, \tag{26}$$

$$\hat{A} = C^{-1}A = \begin{bmatrix} a_{11} & a_{12} & 0 & -g \\ a_{21} & a_{22} & 1 & 0 \\ \hat{a}_{31} & \hat{a}_{32} & \hat{a}_{33} & 0 \\ 0 & 0 & 1 & 0 \end{bmatrix} \quad , \quad \hat{B} = C^{-1}B = \begin{bmatrix} 0 \\ \hat{b}_2 \\ \hat{b}_3 \\ 0 \end{bmatrix} \tag{26a}$$

C is invertible matrix. Therefore it can be move to do right hand side of the Equation (25). Component of the A and B matrix detailed expressions can be obtained from the coefficient linearized longitudinal motion equations for $\dot{v}_p$, $\dot{\alpha}$, $\dot{q}$, $\dot{\theta}$. Equation (26) is given in Equation (27). Some assumptions were made while generating the coefficients in Equation (27) (Howe, 1980). These assumptions are set out below.

- P_z is neglected, the z component of powerplant force
- $C_{L_0} = C_L$
- $C_{M_0} = 0$
- $C_D = C_{D_0} + C_{D_{CL^2}}C_{L_0}$
- $\frac{P_x}{m} = \frac{gC_D}{C_L}$

$$
\begin{aligned}
c_{32} &= -\frac{mgc^2 C_{M_{\dot{\alpha}}}}{2I_{yy}V_{p_0}C_L} & a_{32} &= \frac{mgcC_{M_\alpha}}{I_{yy}C_L} \\
a_{11} &= -\frac{2gC_D}{V_{p_0}C_L} & a_{33} &= \frac{mgc^2 C_{M_Q}}{2I_{yy}V_{p_0}C_L} \\
a_{12} &= g\left(1 - 2C_{D_{CL^2}}C_{L_\alpha}\right) & a_{43} &= 1 \\
a_{14} &= -g & b_2 &= -\frac{g}{V_{p_0}}\frac{C_{L_{\delta_e}}}{C_L} \\
a_{21} &= \frac{-2g}{V_{p_0}{}^2} & b_3 &= \frac{mgcC_{M_{\delta_e}}}{I_{yy}C_L} \\
a_{22} &= -\frac{g}{V_{p_0}}\left(\frac{C_{L_\alpha}}{C_L} + \frac{C_D}{C_L}\right) & \hat{a}_{31} &= -c_{32}a_{21} + a_{31} \\
a_{23} &= 1 & \hat{a}_{32} &= -c_{32}a_{22} + a_{32} \\
a_{31} &= 0 & \hat{a}_{33} &= -c_{32} + a_{33} \\
 & & \hat{b}_3 &= -c_{32}b_2 + b_3
\end{aligned}
\tag{27}
$$

After the coefficients in the matrix are defined, the state variable motion equations can be expressed as in Equation (28-31) as below.

$$\dot{V}_p = a_{11}v_p + a_{12}\alpha + a_{14}\,\theta \tag{28}$$

$$\dot{\alpha} = a_{21}v_p + a_{22}\alpha + q + b_2\delta_e \tag{29}$$

$$\dot{q} = \hat{a}_{32}\alpha + \hat{a}_{33}q + \hat{b}_3\delta_e + \hat{a}_{31}v_p \tag{30}$$

$$\dot{\theta} = q \tag{31}$$

Letting $\dot{q} = sq = s^2\theta$ and $\dot{\alpha} = s\alpha$. Thus, the pitch transfer function, which is the ratio of the pitch angle to elevator displacement resulting from the longitudinal motion and the behavior of the elevator control surface, appears as in Equation (32) and (33) as below.

$$\frac{\theta}{\delta_e}(s) = \frac{(b_3 - c_{32}b_2)s^2 + [b_2(c_{32}a_{11} + a_{32}) - b_3(a_{11} + a_{22})]s + b_3(a_{11}a_{22} - a_{21}a_{12}) - b_2a_{32}a_{11}}{D(s)} \tag{32}$$

where

$$
\begin{aligned}
D(s) = s^4 &+ (c_{32} - a_{11} - a_{22} - a_{33})s^3 + [a_{11}a_{22} - a_{21}a_{12} + a_{33}(a_{11} + a_{22})c_{32}a_{11} - a_{32}]s^2 \\
&+ [c_{32}a_{21}a_{14} + a_{32}a_{11} - a_{33}(a_{11}a_{22} - a_{21}a_{12})]s + a_{32}a_{21}a_{14}
\end{aligned}
\tag{33}
$$

Overall, the transfer function resulting from the longitudinal motion of the aircraft is expressed. Separately, the ratio of the pitch angle to elevator displacement can be introduced in Equations (34) in the following form (Howe, 1980).

$$\frac{\theta}{\delta_e}(s) = K_e \frac{(\tau_s + 1)(\tau_p + 1)}{(\frac{1}{W_{ns}{}^2}s^2 + \frac{2\zeta_s}{W_{np}{}^2}s + 1)(\frac{1}{W_{np}{}^2}s^2 + \frac{2\zeta_p}{W_{np}{}^2}s + 1)} \tag{34}$$

2.3.2. The linearized lateral equations

States of the lateral motions that are side slip angle (β), roll rate (p), yaw rate (r) and bank angle (Φ). Before performing the linearization process, the nonlinear forms of the state are given in Equation (35-37).

$$\dot{\beta} = \frac{F_y}{mV_p} - R \tag{35}$$

$$\dot{p} = \frac{M_x}{I_{xx}} + \left(\frac{I_{yy}-I_{zz}}{I_{xx}}\right) qr + \frac{I_{xz}}{I_{xx}}(pq + \dot{r}) \tag{36}$$

$$\dot{r} = \frac{M_z}{I_{zz}} + \left(\frac{I_{xx}-I_{yy}}{I_{zz}}\right) pq + \frac{I_{xz}}{I_{zz}}(\dot{p} - qr) \tag{37}$$

The linearization process is started by determining the equilibrium points over the nonlinear forms. The equilibrium points of states determined in lateral motion are $\beta = 0, p = 0, r = 0$ and $\Phi = 0$. Thus, the linearized lateral motion Equations for $\dot{\beta}$, $\dot{p}$, $\dot{r}, \dot{\Phi}$ are expressed in Equation (38-41).

$$\dot{\beta} = \frac{gC_{Y_\beta}}{V_{p_0}C_L}\beta - r + \left(\frac{g}{V_{p_0}}\right)\Phi + (\frac{gC_{Y_{\delta_r}}}{V_{p_0}C_L})\delta_r \tag{38}$$

$$\dot{p} = \left(\frac{mgbC_{l_\beta}}{I_{xx}C_L}\right)\beta + \left(\frac{mgb^2C_{l_p}}{2I_{xx}V_{p0}C_L}\right)p + \left(\frac{mgb^2C_{l_R}}{2I_{xx}V_{p0}C_L}\right)r + \frac{I_{xz}}{I_{xx}}\dot{r} + \left(\frac{mgbC_{l\delta_a}}{I_{xx}C_L}\right)\delta_a + \left(\frac{mgbC_{l\delta_r}}{I_{xx}C_L}\right)\delta_r \tag{39}$$

$$\dot{r} = \left(\frac{mgbC_{N_\beta}}{I_{zz}C_L}\right)\beta + \left(\frac{mgb^2C_{N_p}}{2I_{zz}V_{p_0}C_L}\right)p + \left(\frac{mgb^2C_{N_R}}{2I_{zz}V_{p_0}C_L}\right)r + \frac{I_{xz}}{I_{zz}}\dot{p} + \left(\frac{mgbC_{N_{\delta_a}}}{I_{zz}C_L}\right)\delta_a + \left(\frac{mgbC_{N_{\delta_r}}}{I_{zz}C_L}\right)\delta_r \tag{40}$$

$$\dot{\Phi} = p \tag{41}$$

These Equations are specified in the form of vector notation in Equation (42) as follows.

$$C\dot{X} = AX + B\delta \rightarrow \begin{bmatrix} 1 & 0 & 0 & 0 \\ 0 & 1 & c_{23} & 0 \\ 0 & c_{32} & 1 & 0 \\ 0 & 0 & 0 & 1 \end{bmatrix}\begin{bmatrix} \dot{\beta} \\ \dot{p} \\ \dot{r} \\ \dot{\Phi} \end{bmatrix} = \begin{bmatrix} a_{11} & 0 & -1 & a_{14} \\ a_{21} & a_{22} & a_{23} & 0 \\ a_{31} & a_{32} & a_{33} & 0 \\ 0 & 1 & 0 & 0 \end{bmatrix}\begin{bmatrix} \beta \\ p \\ r \\ \Phi \end{bmatrix} + \begin{bmatrix} 0 & b_{12} \\ b_{21} & b_{22} \\ b_{31} & b_{32} \\ 0 & 0 \end{bmatrix}\begin{bmatrix} \delta_a \\ \delta_r \end{bmatrix} \tag{42}$$

where,

$$C = \begin{bmatrix} 1 & 0 & 0 & 0 \\ 0 & 1 & c_{23} & 0 \\ 0 & c_{32} & 1 & 0 \\ 0 & 0 & 0 & 1 \end{bmatrix}, A = \begin{bmatrix} a_{11} & 0 & -1 & a_{14} \\ a_{21} & a_{22} & a_{23} & 0 \\ a_{31} & a_{32} & a_{33} & 0 \\ 0 & 1 & 0 & 0 \end{bmatrix}, B = \begin{bmatrix} 0 & b_{12} \\ b_{21} & b_{22} \\ b_{31} & b_{32} \\ 0 & 0 \end{bmatrix} \tag{43}$$

$$\hat{A} = C^{-1}A = \begin{bmatrix} a_{11} & 0 & -1 & a_{14} \\ \hat{a}_{21} & \hat{a}_{22} & \hat{a}_{23} & 0 \\ \hat{a}_{31} & \hat{a}_{32} & \hat{a}_{33} & 0 \\ 0 & 1 & 0 & 0 \end{bmatrix}, \quad \hat{B} = C^{-1}B = \begin{bmatrix} 0 & b_{12} \\ \hat{b}_{21} & \hat{b}_{22} \\ \hat{b}_{31} & \hat{b}_{32} \\ 0 & 0 \end{bmatrix} \tag{43a}$$

C is invertible matrix. Therefore it can be move to do right hand side of the Equation (42).Component of the A and B matrix detailed expressions can be obtained from the coefficient linearized longitudinal motion Equations for $\dot{\beta}$, $\dot{p}$, $\dot{r}$, $\dot{\Phi}$. Equation (43) is given in Equation (44)

$$
\begin{aligned}
&c_{23} = -\frac{I_{xz}}{I_{xx}} && b_{12} = (\frac{gC_{Y\delta_r}}{V_{p_0}C_L}) \\
&c_{32} = -\frac{I_{xz}}{I_{zz}} && b_{21} = \left(\frac{mgbC_{l\delta_a}}{I_{xx}C_L}\right) \\
&a_{11} = \frac{gC_{Y_\beta}}{V_{p_0}C_L} && b_{22} = \left(\frac{mgbC_{l_{\delta_r}}}{I_{xx}C_L}\right) \\
&a_{14} = \left(\frac{g}{V_{p0}}\right) && b_{31} = \left(\frac{mgbC_{N_{\delta_a}}}{I_{zz}C_L}\right) \\
&a_{21} = \left(\frac{mgbC_{l_\beta}}{I_{xx}C_L}\right) && b_{32} = \left(\frac{mgbC_{N_{\delta_r}}}{I_{zz}C_L}\right) \\
&a_{22} = \left(\frac{mgb^2C_{l_p}}{2I_{xx}V_{p_0}C_L}\right) && \hat{a}_{21} = -\frac{1}{c_{23}c_{32}-1}a_{21} + \frac{c_{23}}{c_{23}c_{32}-1}a_{31} \\
&a_{23} = \left(\frac{mgb^2C_{l_R}}{2I_{xx}V_{p0}C_L}\right) && \hat{a}_{22} = -\frac{1}{c_{23}c_{32}-1}a_{22} + \frac{c_{23}}{c_{23}c_{32}-1}a_{32} \\
&a_{31} = \left(\frac{mgbC_{N_\beta}}{I_{zz}C_L}\right) && \hat{a}_{23} = -\frac{1}{c_{23}c_{32}-1}a_{23} + \frac{c_{23}}{c_{23}c_{32}-1}a_{33} \\
&a_{32} = \left(\frac{mgb^2C_{Np}}{2I_{zz}V_{p0}C_L}\right) && \hat{a}_{32} = \frac{c_{32}}{c_{23}c_{32}-1}a_{22} - \frac{1}{c_{23}c_{32}-1}a_{32} \\
&a_{33} = \left(\frac{mgb^2C_{N_R}}{2I_{zz}V_{p_0}C_L}\right) && \hat{b}_{21} = -\frac{1}{c_{23}c_{32}-1}b_{21} + \frac{c_{23}}{c_{23}c_{32}-1}b_{31} \\
&\hat{a}_{31} = \frac{c_{32}}{c_{23}c_{32}-1}a_{21} - \frac{1}{c_{23}c_{32}-1}a_{31} && \hat{b}_{31} = \frac{c_{32}}{c_{23}c_{32}-1}b_{21} - \frac{1}{c_{23}c_{32}-1}b_{31} \\
&\hat{a}_{33} = \frac{c_{32}}{c_{23}c_{32}-1}a_{23} - \frac{1}{c_{23}c_{32}-1}a_{33} && \hat{b}_{32} = \frac{c_{32}}{c_{23}c_{32}-1}b_{22} - \frac{1}{c_{23}c_{32}-1}b_{32} \\
&\hat{b}_{22} = -\frac{1}{c_{23}c_{32}-1}b_{22} + \frac{c_{23}}{c_{23}c_{32}-1}b_{32}
\end{aligned} \tag{44}
$$

After the coefficients in the matrix are defined, the state variable motion Equations can be expressed as in Equation 45-48 as below.

$$\dot{\beta} = a_{11}\beta - r + a_{14}\Phi + b_{12}\delta_r \tag{45}$$

$$\dot{p} = \hat{a}_{21}\beta + \hat{a}_{22}p + \hat{a}_{23}r + \hat{b}_{21}\delta_a + \hat{b}_{22}\delta_r \tag{46}$$

$$\dot{r} = \hat{a}_{31}\beta + \hat{a}_{32}p + +\hat{a}_{33}r + \hat{b}_{31}\delta_a + \hat{b}_{32}\delta_r \tag{47}$$

$$\dot{\Phi} = p \tag{48}$$

When simplifying the algebra, the new parameters specified in Equation (45) are defined as the coefficients in Equations (49) and (50).

$$
\begin{aligned}
&[s^2 - (a_{11} + a_{33})s + (a_{31} + a_{33}a_{11})]r \\
&\qquad = [-c_{32}s^3 + (a_{32} + c_{32}a_{11})s^2 - a_{32}a_{11}s + a_{31}a_{14}]\Phi + (b_{31}s - b_{31}a_{11})\delta_a \\
&\qquad + (b_{32}s + a_{31}b_{12} - b_{32}a_{11})\delta_r
\end{aligned} \tag{49}
$$

$$
\begin{aligned}
&[(a_{31} - a_{21}c_{32})s^2 + (a_{21}a_{32} - a_{31}a_{32})s]\Phi \\
&\qquad = [(a_{21} - a_{31}c_{23})s + a_{31}a_{23} - a_{21}a_{33}\ ]r + (a_{31}b_{21} - a_{21}b_{31})\delta_a + (a_{31}b_{22} \\
&\qquad - a_{21}b_{32})\delta_r
\end{aligned} \tag{50}
$$

As we simplify the algebra, we define the new parameters specified in Equation (51) as coefficients in Equations (49) and (50).

$$
\begin{aligned}
&a_1 = -(a_{11} + a_{33}) && b_3 = b_{32} \\
&a_0 = a_{31} + a_{33}a_{11} && b_2 = a_{31}b_{12} - b_{32}a_{11} \\
&c_3 = -c_{32} && d_2 = a_{31} - a_{21}c_{32} \\
&c_2 = a_{32} + c_{32}a_{11} && d_1 = a_{21}a_{32} - a_{31}a_{22} \\
&c_1 = -a_{32}a_{11} && k_1 = a_{21} - a_{31}c_{23} \\
&c_0 = a_{31}a_{14} && k_0 = a_{31}a_{23} - a_{21}a_{33} \\
&b_1 = b_{31} && b_4 = a_{31}b_{21} - a_{21}b_{31} \\
&b_0 = -b_{31}a_{11} && b_4 = a_{31}b_{21} - a_{21}b_{31}
\end{aligned}
\tag{51}
$$

Thus, when the lateral motion Equations are examined, the transfer function expressing the ratio of the bank angle according to both aileron and rudder displacement emerges in Equation (52) and (53) as follows.

$$
\Phi(s) = \frac{(b_4+b_1k_1)s^2+[b_4a_1+b_0k_1]s+(b_4a_0+b_0k_0)}{D_1(s)}\delta_a + \frac{(b_5+b_3k_1)s^2+[b_5a_1+b_2k_1+b_3k_0]s+(b_5a_0+b_2k_0)}{D_1(s)}\delta_r \tag{52}
$$

where

$$
\begin{aligned}
D_1(s) = {} & (d_2 - c_3k_1)s^4 + (d_2a_1 + d_1 - c_2\,k_1 - c_3k_0)s^3 + [a_0d_2 + a_1d_1 - c_1k_1 - c_2k_0]s^2 \\
& + [a_0d_1 - c_1k_0 - c_0k_1]s + c_0k_0
\end{aligned}
\tag{53}
$$

In general, the transfer function resulting from the lateral motion of the aircraft is expressed. Separately, the ratio of the bank angle to aileron displacement and rudder displacement can be expressed in Equations (54) and (55) in the following form (Howe, 1980).

$$
\frac{\Phi}{\delta_a}(s) = -K_a \frac{\frac{s^2}{{w_{n\Phi}}^2} + \frac{2\zeta_\Phi s}{w_{n\Phi}} + 1}{(T_{\Phi 1}s + 1)(T_{\Phi 2}s + 1)(\frac{s^2}{{w_{nr}}^2} + \frac{2\zeta_r s}{w_{nr}} + 1)} \tag{54}
$$

$$
\frac{\Phi}{\delta_r}(s) = K_r \frac{(T_{\Phi r_1}s + 1)(-T_{\Phi r_2}s + 1)}{(T_{\Phi 1}s + 1)(T_{\Phi 2}s + 1)(\frac{s^2}{{w_{nr}}^2} + \frac{2\zeta_r s}{w_{nr}} + 1)} \tag{55}
$$

3. ESTIMATION ALGORITHM

Several parameter estimation methods are employed online and offline to eliminate the uncertainties in many systems. Some of them are the maximum likelihood method, least square method (LSM), recursive least square method (RLSM), and time-varying parameters methods (Klein and Morelli, 2006). Since it is a dynamic system in the aviation field and the parameters are updated instantaneously, parameter estimation methods are required in this area. In this paper, the LS method is practiced and demonstrated.

3.1. Least Square Method

The least square is a parameter estimation method that attempts to obtain the approximate solution for a specified function via minimizing the sum of the squares of the residuals computed in every iteration. The least square method considers that the best-fitting curve of a given type is the curve with a minimum deviation sum (Molugaram and Rao, 2017). Assume that the data points are (x_1, y_1), (x_2, y_2), . . . , (x_n, y_n) where x is the independent variable, y is the dependent variable and n is the number of data points. The fitting curve $f(x)$ deviation (error) e_i from each data point, as in Equation (56):

$$\begin{aligned} e_1 &= y_1 - f(x_1), \\ e_2 &= y_2 - f(x_2), \\ &. \\ &. \\ e_n &= y_n - f(x_n) \end{aligned} \tag{56}$$

The sum of the squares of the errors must be minimum in order to define the most suitable curve according to the LS method. The purpose of this method is to solve the systems of Equations (57).

$$\sum_1^n {e_i}^2 = \sum_1^n [y_i - f(x_i)]^2 \tag{57}$$

The general definition of the least squares method is depicted above. Now, it has been attempted to express parametrically in detail. In this paper, the transfer functions are analyzed to find unknown parameters, which is the purpose of the least squares method.
The transfer function, which denotes the input-output relationship, is exhibited in Figure 2 below (Chen and Tomizuka, 2014).

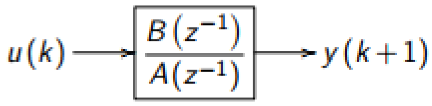

Figure 2. Input-Output Relationship of a Plant (Chen and Tomizuka, 2014)

The numerator and denominator parts of the plant, that is the transfer function, given in Figure 2 are given in Equation (58).

$$B(z^{-1}) = b_0 + b_1 z^{-1} + \cdots + b_m z^{-m}; \qquad A(z^{-1}) = 1 + a_1 z^{-1} + \cdots + a_n z^{-n} \tag{58}$$

$y(k+1)$ is a linear combination of $y(k), \ldots, y(k+1-n)$ and $u(k), \ldots, u(k-m)$ and is expressed in Equation (59).

$$y(k+1) = -\sum_{i=1}^{n} a_i y(k+1-i) + \sum_{i=0}^{n} b_i u(k-i) \tag{59}$$

The transfer function was expressed above. where the $\theta = [a_1, a_2, \ldots a_n, b_0, b_1, \ldots, b_m]^T$ and the regressor vector $\phi(k) = [-y(k), \ldots, -y(k+1-n), u(k), u(k-1), \ldots, u(k-m)]^T$ are the parameter vector that must be defined in the transfer function.The relationship between them as general system modeling is expressed in Equation (60) below.

$$y(k+1) = \theta^T \phi(k) \tag{60}$$

The goal is to estimate unknown parameters θ. The parameter vector to be estimated is $\hat{\theta}^T = \left[\widehat{a_1}, \widehat{a_2}, \dots \widehat{a_n}, \widehat{b_0}, \widehat{b_1}, \dots, \widehat{b_m}\right]^T$.

At time k, unknown parameters in the system can be estimated. The expression in Equation (61) below refers to the system to be estimated.

$$\hat{y}\,(k\ +1)\ = \hat{\theta}^T \phi(k) \tag{61}$$

where

$$\hat{\theta}^T = \left[\widehat{a_1}(k), \widehat{a_2}(k), \dots \widehat{a_n}(k), \widehat{b_0}(k), \widehat{b_1}(k), \dots, \widehat{b_m}(k)\right]^T$$

As stated at the beginning of the subject, the error function J_k defined in Equation (62) must be minimum in order to minimize the error.

$$J_k = \sum_{i=1}^{k} [y(i) - \hat{\theta}^T(k)\phi(i-1)]^2 \tag{62}$$

The result of this expression is given in Equation (63).

$$J_k = \sum_{i=1}^{k} [y(i)^2 + \hat{\theta}^T(k)\phi(i-1)\phi^T(i-1)\hat{\theta}(k) - 2y(i)\phi^T(i-1)\hat{\theta}(k)]^2 \tag{63}$$

The partial derivative must be 0 for the function J_k to be minimum ($\partial J_k / \partial \theta\,(k)\ =\ 0$). As a result of this process, $\hat{\theta}\,(k)$ parameter vector, which is our aim, is found as in Equation (64) by the least squares method.

While θ is found here, the matrix inversion method has been applied. This matrix inversion method can be applied only when the coefficient matrix is a square matrix and non-singular. Thus, ϕ is square and non-singular matrix. If matrix determinant is equal non-zero, this matrix is non-singular. Since ϕ is non-singular, ϕ^{-1} exists and $\phi^{-1}\,\phi =\ \phi\phi^{-1} = I$. Where I is identity matrix ($\phi\theta = y \rightarrow \phi^{-1}(\phi\theta)$= $\phi^{-1}y \rightarrow \theta = \phi^{-1}y$).

$$\hat{\theta}\,(k) = F(k) \sum_{i=1}^{k} \phi(i-1)y(i) \tag{64}$$

where

$$F(k) = \left[\sum_{i=1}^{k} \phi(i-1)\phi^T(i-1)\right]^{-1}$$

As a result, using Equation (64), all parameters are obtained. Thus, derivatives are not taken for each parameter individually. With this expression, each parameter is solved.

4. ESTIMATION OF TRANSFER FUNCTIONS RESULTING FROM THE BEHAVIOR OF AIRCRAFT CONTROL SURFACES WITH LS METHOD

LS methods estimate transfer functions resulting from the behavior of the aircraft control surfaces such as the elevator, aileron, and rudder related to the longitudinal and lateral motion of the aircraft. The resulting transfer functions are examined in the time domain and with their original and predicted form. Graphs are included to comprehend the approach of LS methods with actual data. MATLAB / Simulink program was utilized to establish the algorithm and in the modeling phase of the system. Models are composed for each elevator, aileron, and rudder control surface. In the model created in the MATLAB / Simulink program, a doublet input to the elevator displacement, aileron displacement, and rudder displacement, which is the input of the system, is defined. Doublet inputs are applied to indicate side pulses (Klein and Morelli, 2006). The graph in Figure 3 below can be illustrated as an example of doublet input.

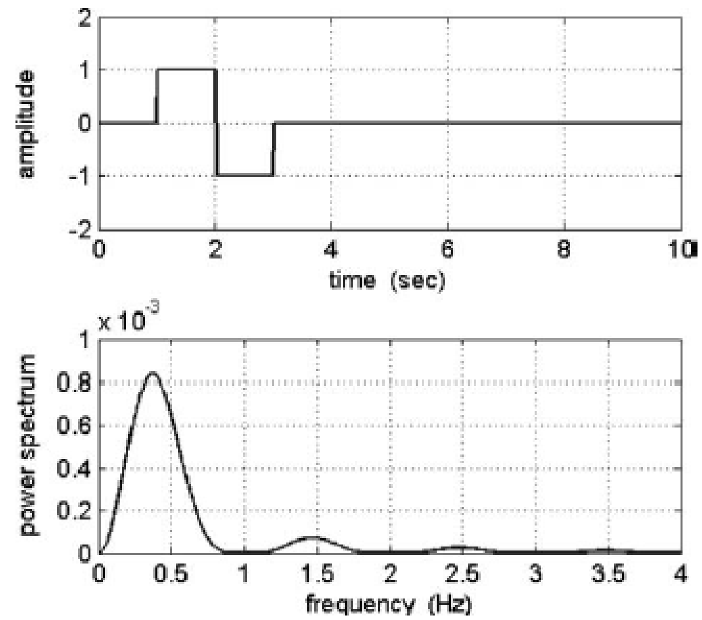

Figure 3. Doublet Input (Klein and Morelli, 2006)

4.1. Elavator Control Surface

This section outlines the estimation of the transfer function associated with the longitudinal motion and the behavior of the elevator control surface. First, the transfer function between the elevator pitch angle and elevator displacement is calculated from the original data. The transfer function is predicted similarly to its original form applying the LS method algorithm and model in Figure 4 formulated in MATLAB / Simulink.

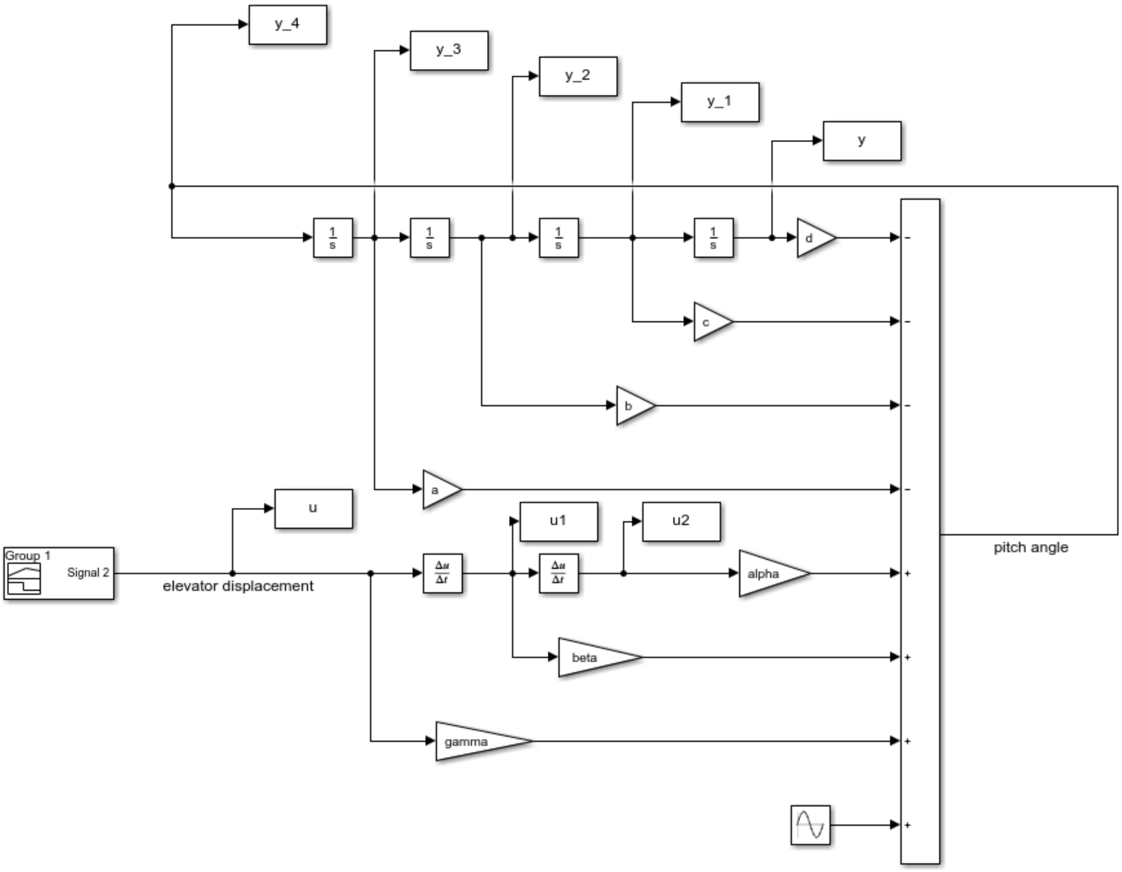

Figure 4. MATLAB/Simulink Model for Elevator Control Surface

Below is the pitch transfer function determined by the original data in Equation (65).

$$\left(\frac{\theta}{\delta_e}\right)_{ORJ} = \frac{-24.7885s^2 - 18.2186s - 0.4659}{s^4 + 2.0072s^3 + 32.5269s^2 + 0.8638s + 0.0179} \tag{65}$$

The algorithm of the least squares method in the MATLAB program and the model in Figure 4 set up in the MATLAB / Simulink program is run. The result is presented in Equation (66).

$$\left(\frac{\theta}{\delta_e}\right)_{LSM} = \frac{-24.7885s^2 - 18.2191s - 0.4447}{s^4 + 2.0072s^3 + 32.5269s^2 + 0.8641s + 0.0176} \tag{66}$$

The transfer function resulting from the behavior of the elevator control surface is estimated with the LS method. The time-domain responses of the estimated and original transfer function are depicted Figure 5 for comparison.

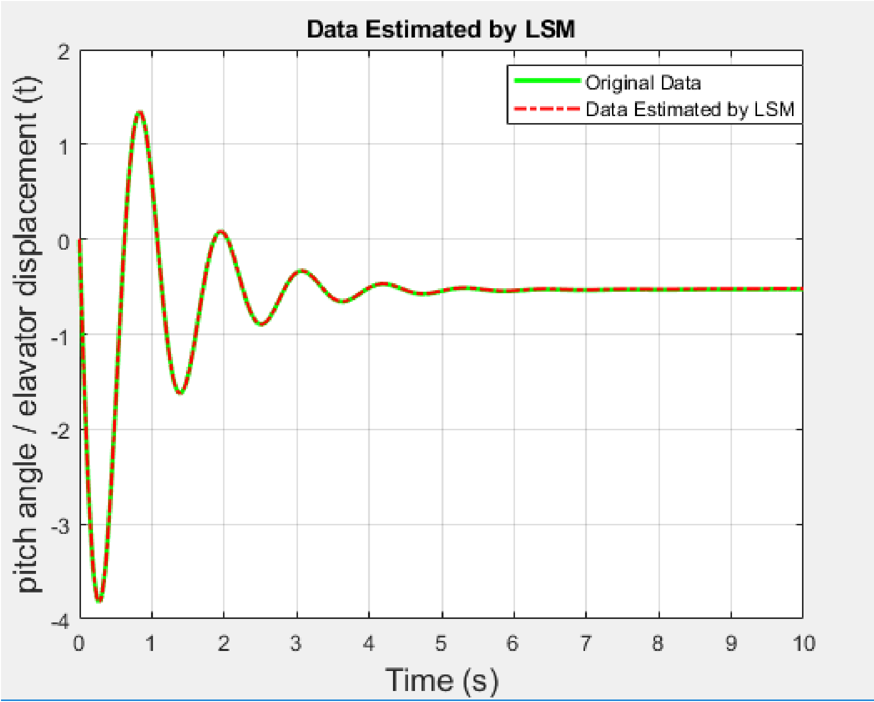

Figure 5. Time Response of Elevator Control Surface Behavior Estimated via LSM

4.2. Aileron Control Surface

This section outlines the estimation of the transfer function associated with the lateral motion and the behavior of the aileron control surface. First, the transfer function between the bank angle and aileron displacement is calculated from the original data. The transfer function is predicted similarly to its original form applying the LS method algorithm and model in Figure 6 formulated in MATLAB / Simulink.

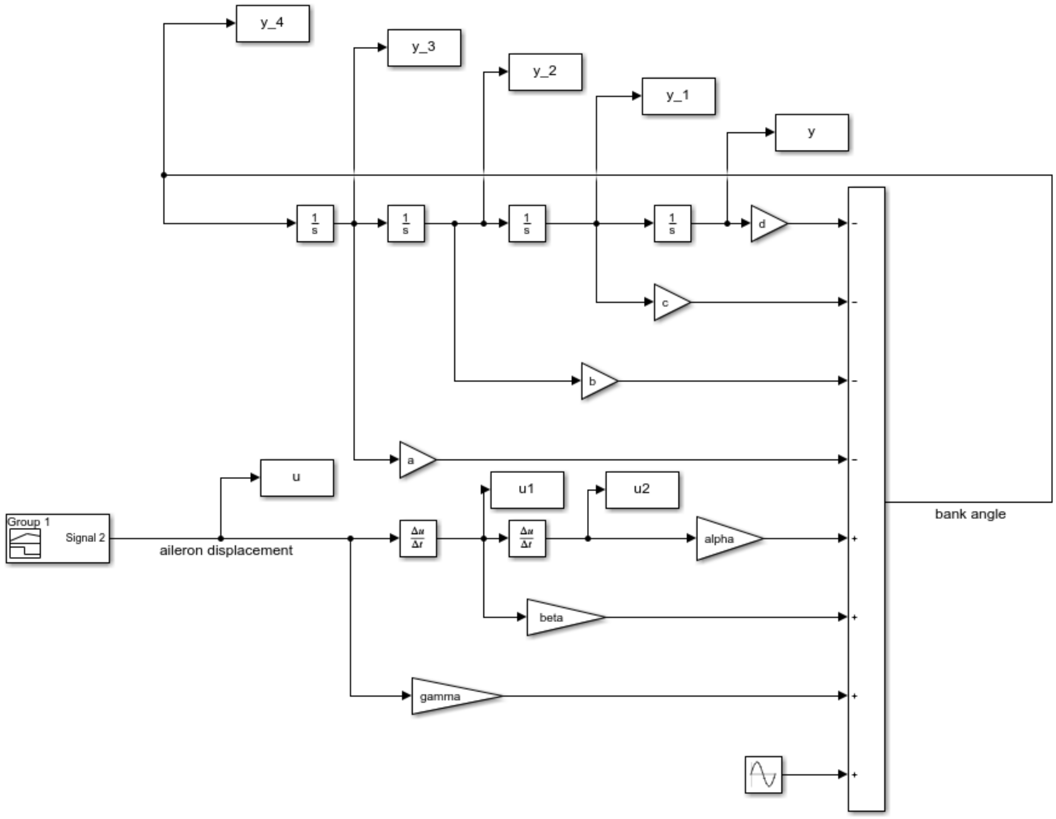

Figure 6. MATLAB/Simulink Model for Aileron Control Surface

Below is the transfer function, which is the ratio of the bank angle to the aileron displacement determined by the original data in Equation (67).

$$\left(\frac{\Phi}{\delta_a}\right)_{ORJ} = \frac{26.8666s^2 + 0.4725s + 94.0527}{s^4 + 1.8683s^3 + 3.6856s^2 + 6.2648s - 0.0085} \tag{67}$$

The algorithm of the least squares method in the MATLAB program and the model in Figure 6 set up in the MATLAB / Simulink program is run. The result is presented in Equation (68).

$$\left(\frac{\Phi}{\delta_a}\right)_{LSM} = \frac{26.8666s^2 + 0.4721s + 94.0737}{s^4 + 1.8683s^3 + 3.6856s^2 + 6.2649s - 0.0087} \tag{68}$$

The transfer function resulting from the behavior of the aileron control surface is estimated with the LS method. The time-domain responses of the estimated and original transfer function are depicted Figure 7 for comparison.

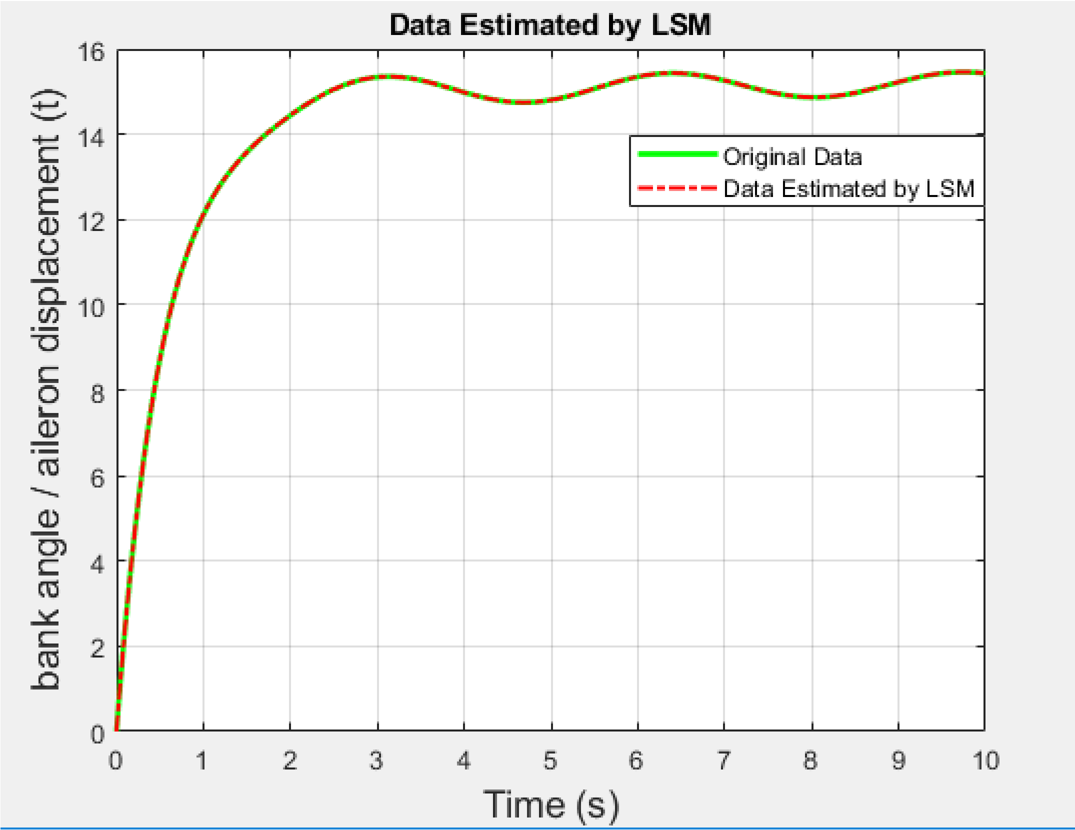

Figure 7. Time Response of Aileron Control Surface Behavior Estimated via LSM

4.3. Rudder Control Surface

This section outlines the estimation of the transfer function associated with the lateral motion and the behavior of the aileron control surface. First, the transfer function between the bank angle and rudder displacement is calculated from the original data. The transfer function is predicted similarly to its original form applying the LS method algorithm and model in Figure 8 formulated in MATLAB / Simulink.

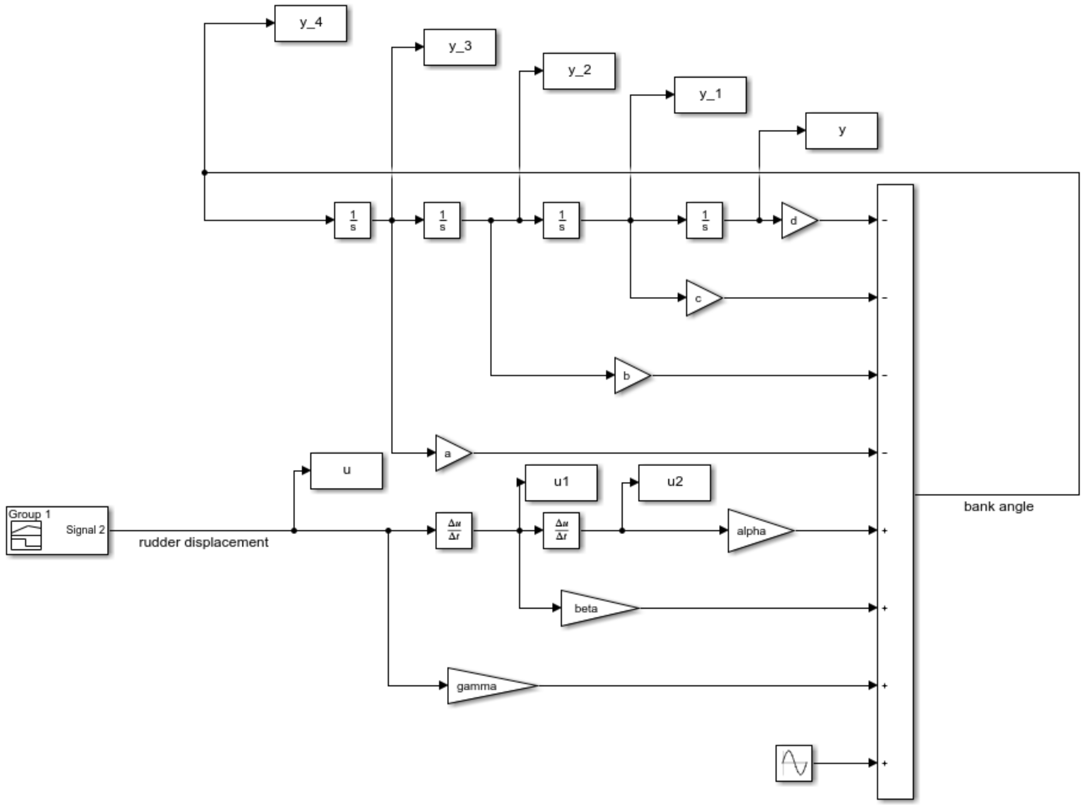

Figure 8. MATLAB/Simulink Model for Rudder Control Surface

Below is the transfer function, which is the ratio of the bank angle to the rudder displacement determined by the original data in Equation (69).

$$\left(\frac{\Phi}{\delta_r}\right)_{ORJ} = \frac{0.5749s^2 - 0.2124s - 4.2481}{s^4 + 1.8683s^3 + 3.6856s^2 + 6.2648s - 0.0085} \tag{69}$$

The algorithm of the least squares method in the MATLAB program and the model in Figure 8 set up in the MATLAB / Simulink program is run. The result is presented in Equation (70).

$$\left(\frac{\Phi}{\delta_r}\right)_{LSM} = \frac{0.5749s^2 - 0.2128s - 4.2263}{s^4 + 1.8678s^3 + 3.6850s^2 + 6.2636s - 0.0031} \tag{70}$$

The transfer function resulting from the behavior of the rudder control surface is estimated with the LS method. The time-domain responses of the estimated and original transfer function are depicted Figure 9 for comparison.

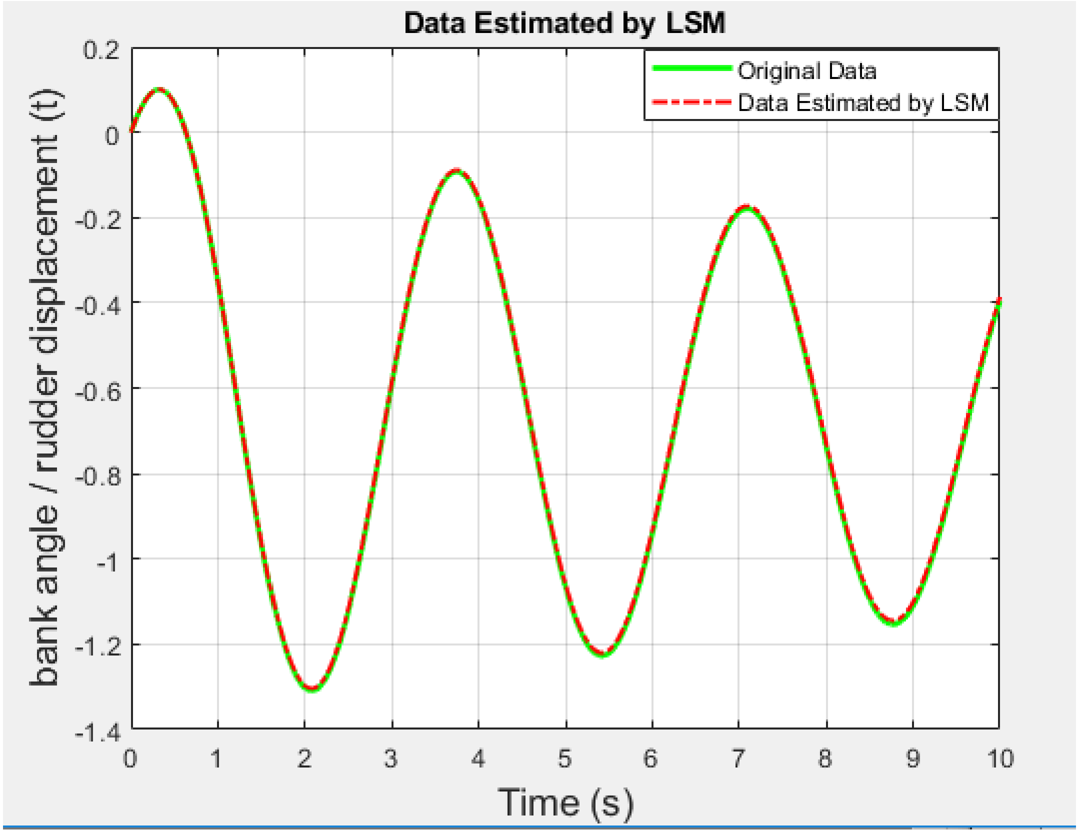

Figure 9. Time Response of Aileron Control Surface Behavior Estimated via LSM

5. ESTIMATION OF AERODYNAMIC PARAMETERS

In section 4, the estimation of transfer functions resulting from the behavior of aircraft control surfaces with the LS method has been explained. In this section, some aerodynamic parameters are obtained using the values of the estimated transfer functions. These estimated aerodynamic parameters are also among the parameters used to derive the original state of the estimated transfer functions. The coefficients of the parametric transfer function found in Equations (32) and (33) were estimated. Consequently, the aerodynamic parameters acquired from the estimation and their original values are presented in Table 1.

Table 1. Estimated of Aerodynamic Parameters

Aerodynamic Paramters	***Original Values***	***Estimated of Least Square***
C_L	0.0642	0.0644
C_D	0.0514	0.0486
C_{M_α}	-0.4	-0.4144
$C_{M_{\dot{\alpha}}}$	-2	-1.9218
C_{L_α}	3	2.974
$C_{D_{CL^2}}$	0.05	0.11
$C_{M_{\delta_e}}$	-0.3	-0.3195
$C_{L_{\delta_e}}$	0.2	0.2006
C_{M_Q}	-8	-4.273

6. CONCLUSION

In this article, the parameter approach, a system definition method, is considered. Accordingly, it was stated that there are many parameter approximation methods online and offline, and the LS method was explained. First of all, mathematical equations of an airplane should be derived to implement a prediction method. In this context, both longitudinal and lateral motion equations are derived in a linearized manner. As a result of the equations achieved, the behavior of airplane control surfaces is analyzed, and transfer functions of their behavior are obtained. These transfer functions formulated with their original values are estimated by the LS method. Graphical outputs were obtained between the original data and the predicted data in the time domain with the models and algorithms applied in the MATLAB / Simulink program.

The time-domain response of the original and estimated transfer functions for all three control surfaces are compared. It is observed that the transfer function predicted by the LS method used presented similar behavior with original data. The input signal for the estimation process is manipulated until the prediction is completed successfully, and the results did not intersect the parameter estimation exactly like the graphs above. In this process, firstly, a single sine sign is applied to the input values, namely elevator, aileron, rudder displacements. This sine value has been applied by implementing various amplitude and frequency values. As a result, estimation performance is not sufficient with this input value. Then again, the application was made to assign the amplitude and frequency of each to the input value as the sum of five sine values by assigning values in different combinations. Again, the prediction is not satisfactory. When the evaluation was made by giving doublet input as the last experiment, the above results were acquired. The estimate process was performed with the LS method with minimum error. In addition, after subtracting the estimated transfer functions, some aerodynamic parameters are extracted and compared with their actual values. An integral Square Error (ISE) table was created to see the error rates of the estimated transfer functions. This ISE table is specified in Table 2. In addition, the error table prepared for the estimated aerodynamic parameters is given in Table 3. It is seen that the algorithm applied using the LS method is close to the actual data. The aerodynamic parameters adopted in these longitudinal motions are addressed in their original form and their estimation state due to the LS method, as shown in Table 1. Consequently, the estimation method is failed to predict the value of C_{M_Q} and $C_{D_{CL^2}}$. Therefore, the prediction process is repeated with the estimated values of C_{M_Q} and C_{M_α} to analyze how the initial value of these parameters result affects the system. While the initial value of C_{M_Q} does not affect the final estimation result, C_{M_α} is influential on the prediction.

In conclusion, it is presented that the LS method may be a sufficient alternative to estimate the aircraft control surface behaviors and aerodynamic parameter estimation.

Table 2. Errors Table for LSM

Parameter Estimation Methods	***Elevator Control Surface (ISE)***	***Aileron Control Surface (ISE)***	***Rudder Control Surface (ISE)***
LSM	0.0001	0.00009	0.000399

Table 3. Error Table for Aerodynamic Parameters

Aerodynamic Paramters	*Error Rates*
C_L	0.00311
C_D	0.0545
C_{M_α}	0.0360
$C_{M_{\dot{\alpha}}}$	0.0391
C_{L_α}	0.0087
$C_{D_{CL^2}}$	1.2
$C_{M_{\delta_e}}$	0.0650
$C_{L_{\delta_e}}$	0.0030
C_{M_Q}	0.4659

Authors' Contribution
The contributions of the authors to the article are equal.

Muammer KALYON contributed to this study in line with his ideas, criticism and method suggestions. Mehmet ŞAHİN contributed to research, application, simulation, analysis, interpretation, literature review and writing of the article.

Acknowledgement
The authors would like to thank Turkish Aerospace Industries Inc. for the working environment provided during the study.

Statement of Interest Conflict
There is no conflict of interest between the authors.

Statement of Research and Publication Ethics
Research and publication ethics were complied with in the study.

REFERENCES

Blakelock, J.H., (1991), Automatic Control of Aircraft and Missiles, Wiley, 672, New Jersey.

Chen, X., Tomizuka, M., (2014). Advanced Control Systems II (Lecture Notes for ME233). University of California, Department of Mechanical Engineering, California.

Gupta, A., (2015), Modeling and Control of an Aircraft System, National Institute of Technology Rourkela, M.Sc. Thesis, 66, Odisha.

Howe, R.M., (1980), Control of Aircraft Missiles and Space Vehicles (Lecture Notes for Aero 574). University of Michigan, Department of Aerospace Engineering, Michigan.

Jategaonkar, R.V., (2006), Flight Vehicle System Identification: A Time Domain Methodology, AIAA (American Institute of Aeronautics & Astronautics), 629, Reston, Virginia.

Klein, V., Morelli, E.A., (2006), Aircraft System Identification: Theory and Practise, AIAA (American Institute of Aeronautics & Astronautics), 484, Reston, Virginia.

Molugaram, K., Rao, G.S., (2017), Statistical Techniques for Transportation Engineering, Elsevier, 554, Amsterdam, Netherlands.

Stevens, B.L., Lewis, F.L., Johnson, E.N., (2016), Aircraft Control and Simulations, Wiley, 749, New Jersey.